The Journal of Experimental Biology 212, 3583-3594
Published by The Company of Biologists 2009
doi:10.1242/jeb.028589

Visual optics and ecomorphology of the growing shark eye: a comparison between deep and shallow water species

Lenore Litherland*, Shaun P. Collin and Kerstin A. Fritsches
Sensory Neurobiology Group, School of Biomedical Science, University of Queensland, Brisbane, QLD 4072, Australia
*Author for correspondence (l.litherland@uq.edu.au)

Accepted 28 July 2009

SUMMARY

Elasmobranch fishes utilise their vision as an important source of sensory information, and a range of visual adaptations have been shown to reflect the ecological diversity of this vertebrate group. This study investigates the hypotheses that visual optics can predict differences in habitat and behaviour and that visual optics change with ontogenetic growth of the eye to maintain optical performance. The study examines eye structure, pupillary movement, transmission properties of the ocular media, focal properties of the lens, tapetum structure and variations in optical performance with ontogenetic growth in two elasmobranch species: the carcharhinid sandbar shark, *Carcharhinus plumbeus*, inhabiting nearshore coastal waters, and the squalid shortspine spurdog, *Squalus mitsukurii*, inhabiting deeper waters of the continental shelf and slope. The optical properties appear to be well tuned for the visual needs of each species. Eyes continue to grow throughout life, resulting in an ontogenetic shift in the focal ratio of the eye. The eyes of *C. plumbeus* are optimised for vision under variable light conditions, which change during development as the animal probes new light environments in its search for food and mates. By contrast, the eyes of *S. mitsukurii* are specifically adapted to enhance retinal illumination within a dim light environment, and the detection of bioluminescent prey may be optimised with the use of lenticular short-wavelength-absorbing filters. Our findings suggest that the light environment strongly influences optical features in this class of vertebrates and that optical properties of the eye may be useful predictors of habitat and behaviour for lesser-known species of this vertebrate group.

Key words: shark, eye growth, ocular media, focal ratio, tapetum, visual ecology.

INTRODUCTION

The visual sense of sharks provides an important source of sensory information, as indicated by the large range of visual adaptations observed in this ecologically diverse vertebrate group (Hart et al., 2006). Optical characteristics of the eye determine the magnification and luminance of the visual image reaching the photosensitive cells of the retina and thereby influence the overall spatial resolution and sensitivity of the visual system. Elasmobranchs and teleosts experience an increase in eye size throughout life (Fernald, 1991; Sivak and Luer, 1991). In teleosts, ocular features have been found to vary with eye growth to avoid compromising visual performance and to adjust to changes in ambient lighting conditions and/or feeding strategies (Fernald, 1991; Shand et al., 1999). Previous authors have investigated optical features of elasmobranch eyes (Sivak, 1974; Sivak, 1976; Sivak and Gilbert, 1976; Sivak, 1978a; Cohen, 1982; Murphy and Howland, 1990; Heath, 1991; Hueter, 1991; Sivak, 1991; Sivak and Luer, 1991; Zigman, 1991; Braekevelt, 1994a; Hueter et al., 2001; Losey et al., 2003; Lisney, 2004; Theiss et al., 2007). However few of these studies have considered the effect of ocular growth on the optical properties of shark visual systems or that some species move between different light environments and thereby have new visual demands placed on the optical apparatus throughout their lifetime (Sivak and Luer, 1991; Fern, 2004; Harahush, 2009).

The present study investigates visual optics in two shark species: the sandbar shark, *Carcharhinus plumbeus* Nardo (Carcharhinidae), and the shortspine spurdog, *Squalus mitsukurii* Jordan and Snyder (Squalidae). Both species have cosmopolitan distributions but occupy dissimilar ecological niches. Environmental light changes with water depth and proximity to land, due to the scattering and absorptive properties of water and the presence of any suspended particulate matter, so each species experiences different visual demands. *Carcharhinus plumbeus* is a highly mobile demersal shark occupying the coastal waters of the neritic province (0–300 m). This species has an extensive distribution ranging from shallow coastal estuaries to offshore continental and insular shelves, such that allopatric populations of *C. plumbeus* experience light conditions that differ in both spectral composition and intensity, depending on habitat depth and water clarity (Springer, 1960; Cliff et al., 1988; Joung and Chen, 1995; Costantini and Affronte, 2003; Joung et al., 2004; McAuley et al., 2005; Romine et al., 2006; Daly-Engel et al., 2007; Grubbs et al., 2007; McAuley et al., 2007). The second species in this study, *S. mitsukurii* is a benthic-associated shark occupying the upper insular and continental slopes of the epipelagic and mesopelagic (200–1000 m) zones of the oceanic province (Wilson and Seki, 1994; Compagno et al., 2005; Graham, 2005). At these depths, sunlight is greatly attenuated and species encounter limited fluctuations in ambient light intensity (Sadler, 1973; Fernald and Wright, 1983). In addition to dim downwelling sunlight, bioluminescent light becomes an important visual cue in the mesopelagic habitat of *S. mitsukurii* (Herring, 1996; Warrant, 2000).

The objective of this study is to characterise the visual optics of *C. plumbeus* and *S. mitsukurii* along an ontogenetic series, from neonates to adults, to ascertain any differences in visual ecology between these two species. We describe ocular dimensions, focal properties of the lens, spectral transmissions of the ocular media, pupil mobility and tapetum structure, to assess whether these key

ocular parameters adapt to different light environments and influence the optical image reaching the retina. We reveal that the visual system of *C. plumbeus* has adapted to facilitate vision in the fluctuating light environment of coastal neritic waters, while *S. mitsukurii* has adapted to maximise light capture in the dim, semi-extended light environment of the mesopelagic zone.

MATERIALS AND METHODS

Source and maintenance of animals

A population of *S. mitsukurii* was sampled (*N*=26) from the insular shelf of the Hawaiian Island chain in the Central Pacific. Three populations of *C. plumbeus* were sampled to represent the extremes in visual environment encountered by this species; a tropical population inhabiting the insular shelf of the Hawaiian Island chain (*C. plumbeus*$_{H1}$; transparent oceanic waters, depth >70 m, *N*=88, TL=50–196 cm), a temperate population inhabiting the continental shelf in the north-western Atlantic Ocean (*C. plumbeus*$_{H2}$; turbid estuarine waters, depth <10 m, *N*=40, TL=55–110 cm) and a subtropical population inhabiting the continental shelf of eastern Australia in the Western Pacific (*C. plumbeus*$_{H3}$; green coastal waters, depth >50 m, *N*=57, TL=50–187 cm) (Table 1). Tissue samples obtained for this study were opportunistically collected from either commercially harvested sharks or from specimens captured for collaborative research projects. Specimens were caught either on rod and reel or on a demersal longline using 14/0 and 18/0 baited circle hooks, set at depths of approximately 300 m (*S. mitsukurii*), 70–100 m (*C. plumbeus*$_{H1}$) and 10 m (*C. plumbeus*$_{H2}$) or donated from commercial longline fishing operations (*C. plumbeus*$_{H3}$). Live animals were sacrificed with either a large dose of benzocaine (Sigma-Aldrich, Inc., St Louis, MO, USA; >250 mg kg^{-1}) or sodium pentobarbital (Beuthanasia-D; Schering-Plough Animal Health Corp., Middletown, PA, USA; >300 mg kg^{-1}). Procedures used in the project have ethical approval from the University of Hawaii: Hawaii Institute of Marine Biology (IACUC 029-07), the College of William and Mary: Virginia Institute of Marine Science (IACUC #0423) and the University of Queensland Animal Welfare Committee (AEC# VTHRC/216/05).

Ocular measurements

The dorsal and nasal limbus of the eyecup was scored for orientation, and the eyes were excised. A series of ocular measurements, along with body measurements of pre-caudal length (PCL), fork length (FL), total length (TL) and information on reproductive maturity, were determined for all individuals. Reproductive maturity in *C. plumbeus* and *S. mitsukurii* was determined by assessing the gonads and, throughout this study, a classification of 'juvenile' refers to immature specimens less than 105 cm TL (*C. plumbeus*) or 40 cm TL (*S. mitsukurii*), 'sub adult' refers to all other immature specimens and 'adult' refers to sexually mature individuals. External eyecup dimensions were measured along the equatorial (i.e. anterior–posterior or A-P), vertical (i.e. dorsal–ventral or D-V) and axial planes and compared as a function of body size. The lens was removed and measured with callipers to the nearest 0.1 mm along the axial, equatorial and vertical planes.

To investigate intraocular morphology, whole enucleated eyes were frozen either in liquid nitrogen or in a –20°C freezer. The robust cartilaginous sclera largely prevented distortion of eye shape during the freezing process; however, particular care was taken so that eyes were not resting on a flat surface, and the smaller eyes of neonatal *S. mitsukurii* were frozen *in situ* within the chondrocranium. The eyecup was never observed to rupture due to increased intraocular pressure from the freezing process. Each frozen eye was mounted in OCT compound (Tissue-Tek; Sakura Finetechnical Co., Tokyo, Japan) and stained with blue Quill Ink in order to provide contrast between the eye and the embedding medium. Eyes were orientated for sectioning along either the equatorial or vertical planes, and frozen sections were cut every 20 µm with a cryostat [Leitz 1720 digital kryostat; Leitz (Leica), Nusslock, Germany] and discarded. Images of the block face with a scale bar were photographed with a digital camera (Canon Powershot s31s) every 200 µm. The photograph with the greatest lens thickness in either the vertical or equatorial planes was deemed to represent the central geometric plane of the lens and therefore to represent the optical axes. Measurements of all intra- and extraocular dimensions were made using Image J freeware (v. 1.3.1; freeware at http://rsb.info.nih.gov/ij/). Measurements were calibrated using the scale bar present in each image. A line joining the centre of the lens to the centre of the pupil was taken to represent the geometric axial axis of the eye (Sivak, 1976). Sections along the equatorial plane revealed anterior (A), posterior (P) and axial visual axes while sections along the vertical plane revealed dorsal (D), ventral (V) and axial visual axes.

In the cryosectioned eye, lens diameter was measured along the equatorial, vertical and axial planes. Lens shape was then established from the ratios of lens diameter (axial:vertical and axial:equatorial). The distance from the centre of the lens to the retina–choroid border was measured along five visual axes (D, V, A, P and axial). The focal ratio (*fr*) of the cryosectioned eye was calculated by dividing the measured distance along the axial axis by the lens radius (hereafter termed fr_1).

Focal properties of the lens

Focal properties of shark lenses were investigated using a custom-made ray tracing apparatus to record the refracted path of a laser beam as it passes through the lens (Kroger et al., 1994). Freshly excised lenses were placed on a stage in a chamber filled with shark saline solution (9 g l^{-1} NaCl; Sigma-Aldrich, Inc., USA) to which a small amount of polymer solution (Polystyrene Microparticle;

Table 1. Overview of sampling populations

Species	Sample location	Habitat type	Capture depth (m)	Sample number	Size range TL (cm)
Sandbar shark (*C. plumbeus*$_{H1}$)	Habitat 1: Central Pacific (Hawaiian Islands)	Oceanic fringing reef	70–100	88	50–196
Sandbar shark (*C. plumbeus*$_{H2}$)	Habitat 2: North-western Atlantic (Virginia's Eastern Shore)	Shallow turbid estuary	6–12	40	55–110
Sandbar shark (*C. plumbeus*$_{H3}$)	Habitat 3: Western Pacific (Australia's eastern seaboard)	Offshore coastal waters	30–50	57	50–187
Shortspine spurdog (*S. mitsukurii*)	Habitat 1: Central Pacific (Hawaiian Islands)	Oceanic insular shelf	250–300	26	39–86

Kisker, Germany) was added to enhance visibility of the helium–neon laser beam. The lens was orientated on the stage so the chamber mimicked the eyecup, with the laser beam tracing through the equatorial plane of the lens. The paths of a green laser (532 nm; Leadlight Technology, Inc., Tao-Yuan, Taiwan) and a red laser (650 nm; Leadlight Technology, Inc.) were traced separately through the lens along the equatorial plane, while filmed from above (dorsal view) with a digital camera (Sony 120X Carl Zeiss, Sony Corp., Tokyo, Japan). Digital film was cut (using imovie, Mac OS X), and individual frames of the video clip were overlaid in Photoshop (Adobe software v. 7.0) to identify the lens focal length (distance from the centre of the lens to the point of laser beam convergence). To investigate the presence and to quantify any chromatic aberration of the lens, the focal lengths of the red and green laser traces were compared. In addition, comparing the convergence distance for a pair of central *vs* peripheral beams enabled a broad assessment of spherical aberration.

The focal ratio of the lens (fr_2=mean focal length of the lens:lens radius) was calculated and compared with values of the focal ratio measured from cryosectioned eyes (fr_1) in order to determine whether this relationship (and therefore the level of retinal illumination) is constrained during eye growth.

Spectral transmission of ocular media

The spectral transmission of light (250–750 nm) through the ocular media was measured separately from the fresh lens, vitreous and cornea, using an S2000 fibre optic spectrometer (Ocean Optics, Dunedin, FL, USA) and a UV-Visible spectrophotometer (Bio-spec 1601; Shimadzu Corp., Kyoto, Japan). An average of three scans was performed for each transmission measurement and normalised to 100% transmission at 700 nm. The wavelength at which transmission reached 50% of the normalised transmittance for each ocular component was considered the transmission cut off (T_{50}) (Douglas and McGuigan, 1989).

Pupillary movements

The dynamic mobility of the pupillary aperture was investigated in live sharks. Live sandbar sharks (N=5 *C. plumbeus*$_{H1}$; N=5 *C. plumbeus*$_{H2}$) were transported from fishing locations in aerated seawater tanks (1000 liter) to land-based aquaria (3000 liter) fitted with flow-through seawater systems and maintained for 4–7 days under a natural light/dark cycle prior to conducting experiments measuring pupil mobility. By contrast, measurements of pupil mobility were conducted on live *S. mitsukurii* (N=2) immediately post capture at sea. Live animals were anaesthetised [25–50 mg l^{-1} benzocaine (Sigma-Aldrich, Inc., USA) or 0.1 ml kg^{-1} ketamine hydrochloride intramuscular injection (Butler Animal Health USA)], artificially ventilated (0.5–1 l min^{-1} kg^{-1}) and dark adapted for 30–60 min. Dark-adapted eyes were exposed *in situ* to a broad-spectrum white light (1.64×10^3 cd m^{-2}), and subsequent pupillary movement was monitored and filmed (including a reference scale) using a digital camera (Sony 120X Carl Zeiss, Sony Corp., Japan or a Sony Cybershot P200, Sony Corp., Japan). Digital film footage was analysed in imovie (Mac OS 10.4) to capture still frames at 0, 0.5, 1, 2, 3, 4, 5, 6, 7, 8, and 30 min time intervals post exposure to light. The pupil area, together with the width of the pupillary aperture, was measured along the equatorial and vertical planes.

Characteristics of the choroidal tapetum

To determine the distribution and colour of the tapetal reflection from the fundus, tapetal reflectance was photographed (Sony Cybershot P200) in light (LA)- and dark-adapted (DA) eyes in *C. plumbeus* (*C. plumbeus*$_{H1}$, N=15 LA and DA; *C. plumbeus*$_{H2}$, N=15 LA and DA) and *S. mitsukurii* (N=2 DA, N=15 LA). Camera settings and lighting conditions were standardised between individuals. The ultrastructure of central regions of the eyecup was examined using electron microscopy to ascertain the mechanism(s) underlying the tapetal reflection. Pieces of retinal tissue (1 mm^2), including the tapetal tissue adjacent to Bruch's membrane, were sampled from central regions of dark- and light-adapted eyes (*C. plumbeus*$_{H1}$, N=5 LA and DA; *C. plumbeus*$_{H2}$, N=5 LA and DA; *S. mitsukurii*, N=2 LA and DA) and processed for light and transmission electron microscopy (TEM). Samples were embedded in Araldite® (Selleys, Padstow, NSW, Australia) and sections were cut on an LKB rotary ultramicrotome (LKB, Uppsala, Sweden) using glass knives. Semi-thin sections were stained with Toluidine Blue, examined under light microscopy and photographed using a Tucsen 5.0 MP camera (Optem, DC500U, Tucsen, Fujian, China) mounted on a light microscope (Olympus BX50). Ultrathin sections were placed on a grid and stained with lead citrate and uranyl acetate (Braekevelt, 1994a). Sections were examined and photographed on either a Phillips 410 or a Phillips CM10 transmission electron microscope set at 80 kV (Phillips Inc., Eindhoven, The Netherlands).

RESULTS

Ocular morphology and eye growth

The eyes of *C. plumbeus* are laterally positioned within the chondrocranium, slightly anterior to the mouth (Fig. 1A). The eyecup of *C. plumbeus* is relatively symmetrical around the axial axis in both the vertical (Fig. 1C) and equatorial planes (Fig. 1E). The eyes of *S. mitsukurii* are positioned laterally, proximal to the rostrum (Fig. 1B). In contrast to *C. plumbeus*, the eyecup of *S. mitsukurii* is asymmetrical around the axial axis in the vertical plane (Fig. 1D) and is positioned within the chondrocranium such that the eye is angled dorso-laterally.

The eyes of *C. plumbeus* and *S. mitsukurii* continue growing throughout life (Fig. 2). The relationship between eye growth and body length did not significantly differ between the three populations of *C. plumbeus* (P>0.05) and so eye size as a function of body size was pooled for interspecific comparisons. *S. mitsukurii* shows an absolute larger eye than *C. plumbeus* for an equivalent body size (P<0.0001, unpaired t-test). In both species, the equatorial (A-P), vertical (D-V) and axial lengths of the eyecup increase in a linear relationship with total body length (Fig. 2A,B). Eye growth is proportional along each plane in *S. mitsukurii*, showing no significant difference between slopes (P=0.1046, one-way ANOVA) (Fig. 2A), but the length of the eyecup in the equatorial plane is consistently longer than the length of the eyecup in the axial plane (P=0.0308, N=25, unpaired t-test). By contrast, eye growth in *C. plumbeus* is allometric (Fig. 2B), with the length of the eyecup in the vertical and equatorial planes increasing at a faster rate than in the axial plane (P<0.0001, N=185, one-way ANOVA). This allometric growth results in a broader, flatter eyecup in an adult *C. plumbeus* compared with a juvenile.

The axial length of the lens in both *C. plumbeus* and *S. mitsukurii* also increases in a linear relationship with body length (Fig. 2C). The slopes are significantly different between the species, indicating that, for an equivalent body size (TL), *S. mitsukurii* has a larger lens than *C. plumbeus* (P<0.0001, N=96, unpaired t-test).

Lens shape in *S. mitsukurii* is relatively spherical as the axial lens length is, on average, only 3±1% shorter than the vertical (D-V) or equatorial (A-P) length. There is no significant change in lens shape during growth (Fig. 2D, P=0.66). By contrast, lens shape in *C. plumbeus* changes as a function of ontogenetic growth, following

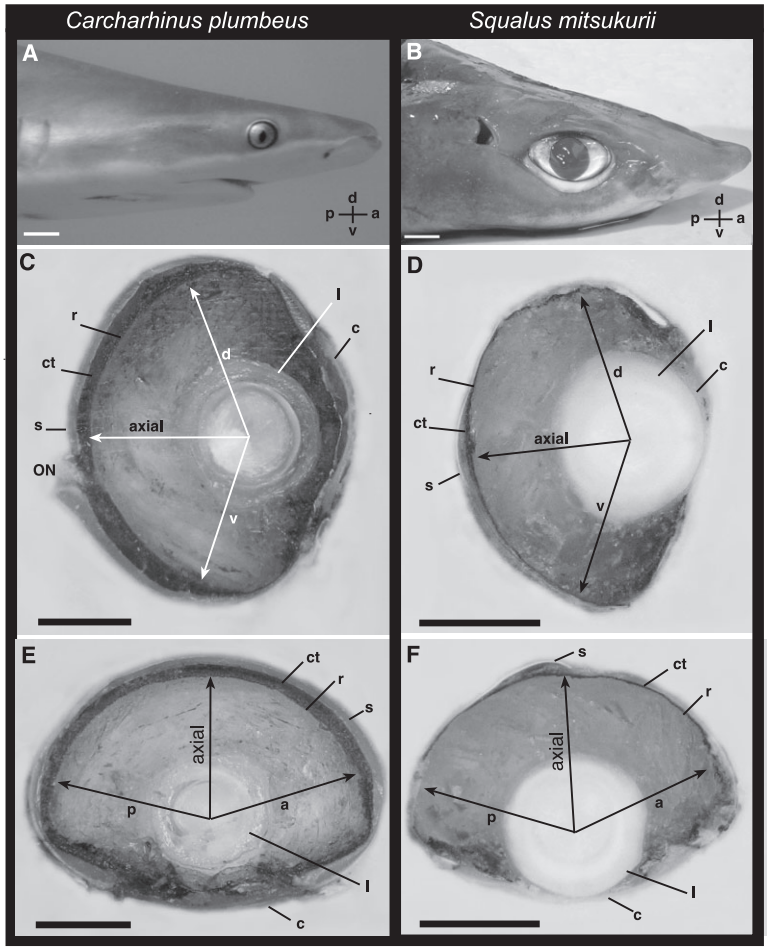

Fig. 1. Ocular structure of *C. plumbeus* (A,C,E) and *S. mitsukurii* (B,D,F). (A,B) Position of the eyes within the chondrocranium. (C,D) Frozen sections through the geometric centre of the eye, sectioned along the vertical plane. Note that the acute curve of the ventral eyecup margin, compared with the dorsal eyecup margin, creates a vertical asymmetry around the axial axis in *S. mitsukurii* (D). (E,F) Frozen sections through the geometric centre of the eye along the equatorial plane. Scale,10 mm. Abbreviations: d, dorsal axis; v, ventral axis; axial, axial axis; a, anterior axis; p, posterior axis; ON, optic nerve; r, retina; c, cornea; l, lens; ct, choroidal tapetum; s, sclera.

a linear relationship that differs significantly from zero (Fig. 2D, R^2=0.65, P<0.0001, N=60). In juvenile *C. plumbeus*, the axial lens length is, on average, 15±0.5% shorter than the vertical or equatorial length (TL=55–65 cm, N=10), giving it an elliptical shape. In adult *C. plumbeus,* the lens approaches a spherical shape with the axial lens length 6.5±0.9% shorter than both the vertical and equatorial length (TL=185–196 cm, N=10).

Focal length and focal ratio

Focal length of the lens (calculated from laser beam convergence) differs from the distance between the centre of the lens and the retina–choroid border (measured in cryosectioned eyes). The focal length of the lens is 8% longer than the measured distance between the lens centre and the retina along the longest axis in *C. plumbeus* (P=0.01, N=58, unpaired t-test) and 10.5% longer in *S. mitsukurii* (P=0.01, N=16, unpaired t-test). Consequently, values of focal ratio calculated from cryosectioned eyes (fr_1) differ marginally from values obtained from the focal properties of the lens (fr_2). Regardless, both calculations ($fr_{1\&2}$) identify a decreasing focal ratio with growth, revealing that eyecup growth does not constrain the optical performance of the lens in *S. mitsukurii* or *C. plumbeus*. In *C. plumbeus*, the focal ratio of the lens (fr_2) decreases with increasing lens size, from approximately 3.3:1 (lens diameter=6.1 mm; TL=65 cm), 2.8:1 (lens diameter=8.1 mm; TL=100 cm) and 2.7:1 (lens diameter=13.8 mm; TL=196 cm). In *S. mitsukurii*, fr_2 also decreases with growth of the eye, but to a smaller extent, from approximately 2.9:1 (lens diameter=6.0 mm; TL=39 cm) to 2.5:1 (lens diameter=7.5mm, TL=48 cm) and 2.4:1 (lens diameter=12.3 mm; TL=86 cm). The decrease in $fr_{1\&2}$ with growth indicates that, in both species, the lens is growing proportionately faster than the focal length. Consequently, the species-specific measures of focal ratio differ significantly (P<0.0001, N=58, one-way ANOVA) (Fig. 3) from Matthiessen's hypothetical focal ratio, a constant of 2.6:1 (Matthiessen, 1882).

Optical aberrations of the lens

Chromatic aberration in the lenses of *C. plumbeus* and *S. mitsukurii* appears to be largely neutralised, with no significant difference between focal lengths of the red (650 nm) and green (532 nm) lasers measured for any lens size. The lenses of *S. mitsukurii* and *C. plumbeus* also appear well corrected (neutralised) for longitudinal spherical aberration (LSA). There was no statistically significant difference between the measured focal lengths of peripheral and central beams (P>0.05), and all beams focus to a narrow focal area (Fig. 4). However, a more detailed analysis of LSA in shark lenses is warranted.

Spectral transmission properties of the ocular media

The analysis of spectral transmittance of the components of the ocular media (cornea, lens and vitreous) for light between 250 and 750 nm reveals that light transmittance is limited primarily by the lens in both *C. plumbeus*$_{H1\&H2}$ and *S. mitsukurii* (Fig. 5). The lens of *S. mitsukurii* blocks light at a longer wavelength (T_{50}=403 nm) than that of *C. plumbeus*$_{H1\&H2}$ (T_{50}=311–384 nm). While no difference in lens transmission is shown between juvenile and adult *S. mitsukurii*, the lens transmission properties of *C. plumbeus*, within

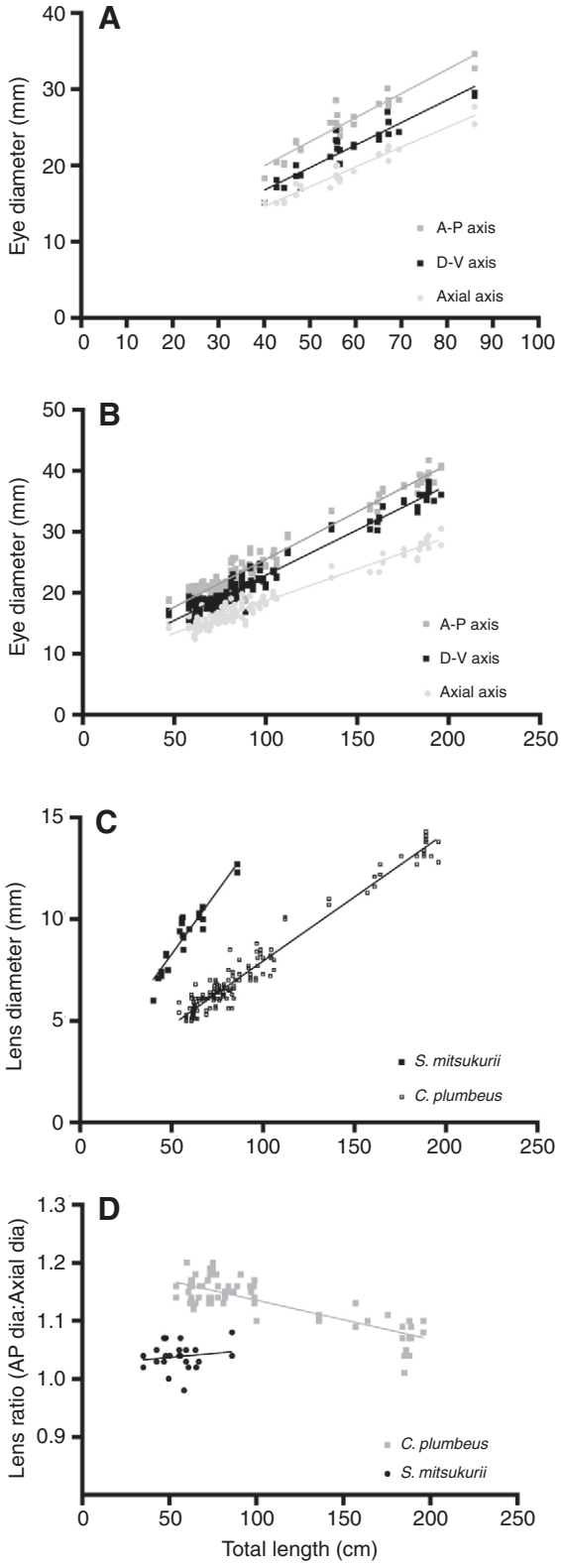

Fig. 2. Growth of the eye and lens. (A) Graph showing the linear increase in eye size with ontogenetic growth in *S. mitsukurii* (A-P, R^2=0.91, y=7.3+0.32x, N=26; D-V, R^2=0.89, y=4.9+0.3x, N=26; axial, R^2=0.94, y=4.2+0.26x, N=25). Growth rate is proportional between the measured axes, with the A-P axis significantly longer than the axial axis (P=0.0308, unpaired t-test). (B) Graph showing linear increase in eye size with ontogenetic growth in *C. plumbeus* (A-P, R^2=0.97, y=9.89+0.16x, N=185; D-V, R^2=0.96, y=8.06+0.15x, N=185; axial, R^2=0.94, y=8.14+0.11x, N=152). Growth is allometric, with a significant difference between the measured axes (P<0.0001, one-way ANOVA). (C) The axial lens diameter increases with body length (TL) in a linear relationship for *S. mitsukurii* (R^2=0.89, y=2.04+0.12x, N=24) and *C. plumbeus* (R^2=0.96, y=1.65+0.06x, N=154). Note the significantly larger lens (and eye) size of *S. mitsukurii* to *C. plumbeus* (P<0.0001, unpaired t-test) for equivalent body size (TL). (D) Change in lens shape as a function of body size (TL). The lens of *S. mitsukurii* maintains its shape with growth (R^2=0.01 is not significantly different from zero; P=0.66). Lens shape is almost spherical with a 3% difference between axial and A/P lens lengths. Lens shape in *C. plumbeus* varies with growth (R^2=0.65, y=1.2+–0.01x; N=72), declining from a 15% (juvenile) to 6% (adult) difference between the axial and A/P lens length.

a single population, vary as a function of body size (Fig. 5C). Juvenile lenses from clear (*C. plumbeus*$_{H1}$) and turbid (*C. plumbeus*$_{H2}$) water habitats have a T_{50} of 311±0.8 nm (TL=65 cm, N=5) and 312±1.2 nm (TL=65 cm, N=2), respectively. This increases to a T_{50} of 384±3.8 nm in the largest individuals sampled (TL=142 cm, N=2, *C. plumbeus*$_{H1}$).

Characteristics of the iris and pupil aperture

Pupillary movement differs between the two species. *C. plumbeus* has a mobile pupil that constricts on exposure to bright light (Fig. 6). While we acknowledge that the rate of pupil movement may have been influenced by the use of anaesthetics, the rates recorded do fall within the range previously reported for elasmobranchs (Kuchnow 1971; Gilbert et al., 1981). The fully dilated pupil forms an almost circular aperture [equatorial:vertical=1:1.14±0.02 (mean ± s.e.m.); N=15], which constricts to a vertical 'keyhole' slit (equatorial:vertical=1:3.31±0.13; N=15) in the light-adapted eye (Fig. 6B,C). This allows the pupil aperture to reduce to half of its maximum dilated area within 1 min of exposure to bright light. Maximum pupil constriction occurs within 5 min of exposure to bright light and is followed by a slight re-dilation (Fig. 6D). At maximum constriction, the pupil aperture is at least 70% smaller than the maximum dilated pupil aperture. The mobile pupil allows for a variable depth of focus and light-gathering power (f-number = lens focal length/pupillary aperture diameter) between light- (f-number=6.0) and dark-adapted (f-number=2.0) eyes. In contrast to *C. plumbeus,* exposure to bright light for 30 min after dark adaptation does not elicit any appreciable pupillary movement in *S. mitsukurii* (Fig. 6A,D). In both the light- and dark-adapted eye of *S. mitsukurii,* the pupil forms a circular aperture (Fig. 6A) with a ratio between the equatorial:vertical aperture widths of 1:1.01±0.02 (mean ± s.e.m.; N=28). Furthermore, no pupillary movement is observed post enucleation, as is the case in *C. plumbeus*. The pupil area of an adult *S. mitsukurii* (TL=86 cm) is 78% larger than the pupil area of a juvenile (TL<40 cm). The static pupillary aperture results in a short depth of focus and thus a high light-gathering power for both juvenile (f-number=1.5) and adult (f-number=1.2) *S. mitsukurii*.

The iris pigmentation of *S mitsukurii* is golden and brightly reflective (Fig. 7). By contrast, ocular pigmentation is observed to vary between populations of *C. plumbeus*. The greatest contrast in iris pigmentation is shown between *C. plumbeus*$_{H1}$ (insular shelf population), where the iris is pale blue to white, and *C. plumbeus*$_{H2}$ (coastal estuary population), where the iris is dark tan or bronze (Fig. 7).

Characteristics of the choroidal tapetum

The coloured reflection elicited from the reflective tapetum in dark-adapted eyes of *C. plumbeus* differs between sampling populations. The greatest contrast is observed between juvenile *C. plumbeus*$_{H1}$,

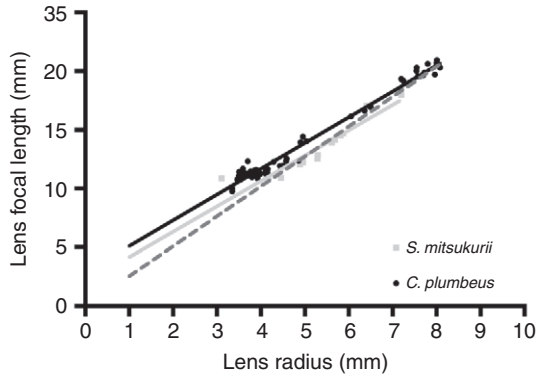

Fig. 3. Focal length as a function of lens radius reveals a linear relationship in *C. plumbeus* (R^2=0.98, y=2.93+2.2x, N=58) and *S. mitsukurii* (R^2=0.89, y=1.2+2.17x, N=16), which differs from Matthiessen's ratio. Broken line represents Matthiessen's ratio (f=2.55r). Note that Matthiessen's ratio gives a close approximation of focal length for large (adult) lenses but not for small (juvenile) lenses.

which have a blue eyeshine, and juvenile *C. plumbeus*$_{H2}$, which have a yellow–green eyeshine (Fig. 7). In *S. mitsukurii*, the tapetum is distributed across the entire fundus and exhibits a blue eyeshine in dark-adapted eyes (Fig. 7).

Ultrastructural analysis of the retina–choroid layers reveals that the source of the observed coloured reflections is a choroidal tapetum (thickness=35.1±0.1 μm in *C. plumbeus*, and 30.3±0.2 μm in *S. mitsukurii*), situated posterior to the choriocapillaris (Fig. 8). The tapetal cells are separated by flattened melanocytes, which contain rounded melanosomes (0.2–0.7 μm in diameter).

The tapetal cell nucleus is found adjacent to the choriocapillaris, and tapetal cells are packed with layers of hexagonal crystals. The tapetal cells in *C. plumbeus* vary in shape depending on the position within the retina. In the central retina, tapetal cells are broad, i.e. ~32.5±0.5 μm×27.8±0.2 μm (means ± s.e.m.), and the crystals are aligned almost horizontally to the mono-layered array of retinal pigment epithelial cells. Away from the central retina, the cells are narrow and elongate, about 9.7±0.8μm×40.4±0.2 μm, with the crystals aligned at an angle approaching 45° to the incident light path (as measured from a perpendicular line through the retinal pigment epithelium and the pupil centre). Where visible, the reflective crystals measured 0.1 μm in thickness and 6–9 μm in length (Fig. 8). Inter-crystal spacing (0.2–0.7 μm) and the number of crystals within each tapetal cell (8–25) show no significant difference between groups due to high inter-individual variation (one-way ANOVA, P>0.05).

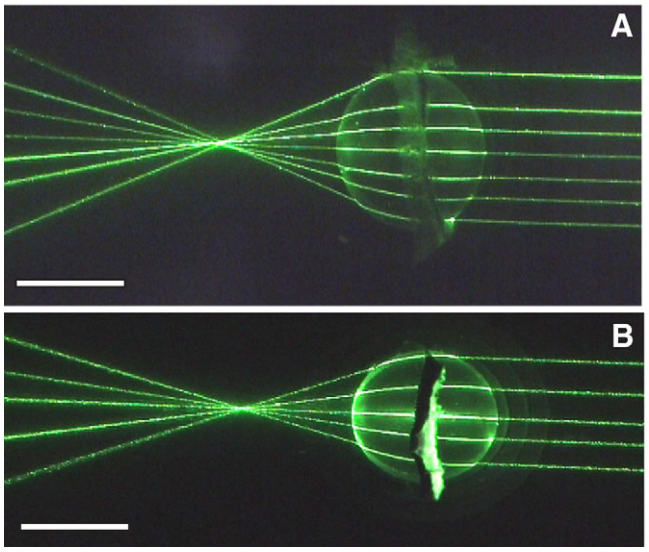

Fig. 4. Focal effects of the lens. Composite image showing the ray traces of a laser beam (532 nm) through a freshly excised lens of (A) *C. plumbeus*$_{H1}$ and (B) *S. mitsukurii*. Note that light is concentrated in a narrow focussed area, indicating that the lens is of a high optical quality and well corrected for spherical aberration. Scale bar, 10 mm.

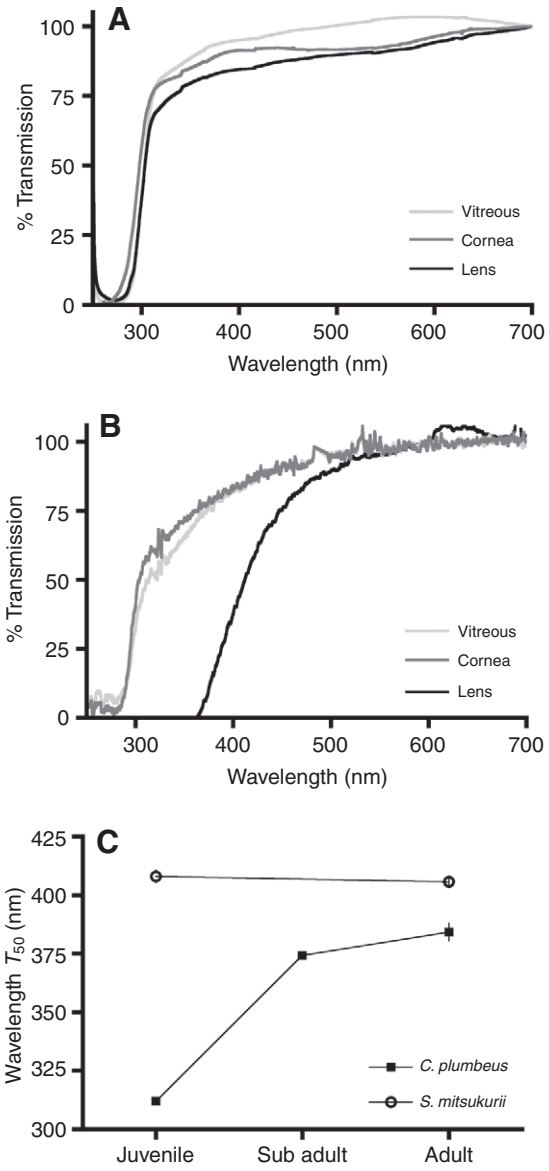

Fig. 5. Spectral transmission properties of the ocular media. Representative transmission curves of light (250–700 nm) through the cornea, lens and vitreous for (A) *C. plumbeus*$_{H2}$ and (B) *S. mitsukurii*. The lens is the limiting factor for light transmission in both species. (C) Graph depicting the mean (± s.d.) light transmission values (T_{50}) as a function of ontogenetic growth. *C. plumbeus* juvenile$_{H1\&H2}$ (TL=65 cm, N=6), sub adult$_{H1}$ (TL=110 cm, N=3), adult$_{H1}$ (TL=142 cm, N=2) and *S. mitsukurii* juvenile (TL=39 cm, N=2) and adult (TL=86, N=2). Transmission properties vary as a function of lens size for *C. plumbeus*$_{H1}$, with larger lenses exhibiting a longer wavelength cut off. *S. mitsukurii* displayed no marked variation in T_{50} with lens growth.

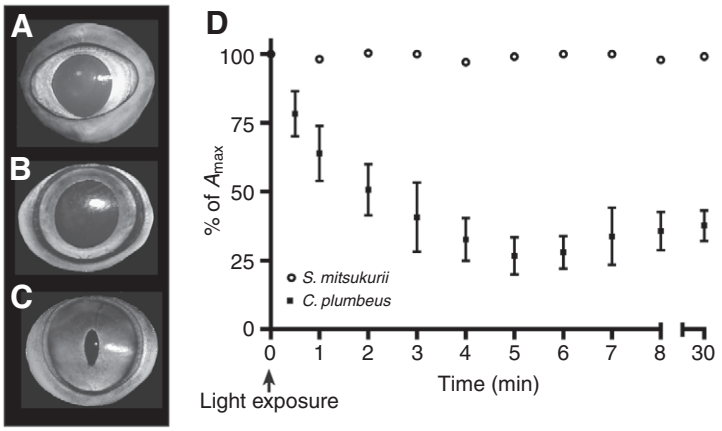

Fig. 6. Pupillary movements with exposure to bright light. (A) The circular pupillary aperture of *S. mitsukurii* did not constrict with exposure to bright light. (B) The circular pupillary aperture of *C. plumbeus*$_{H2}$ after one hour of dark adaptation. (C) The pupil of *C. plumbeus*$_{H2}$ constricts with light adaptation to a 'keyhole' slit. (D) Time course of the pupillary response in *C. plumbeus*$_{H1\&H2}$ and *S. mitsukurii* plotted as the relative pupillary aperture as a function of maximum pupillary aperture (% of A_{max}). Mean values are provided for *S. mitsukurii* (N=2) and *C. plumbeus* (N=10). Note the slight re-dilation of the pupillary aperture in *C. plumbeus* after maximum pupil constriction is reached. No measurable pupil constriction occurs in *S. mitsukurii* over the same timeframe. Onset of light exposure occurs at time=0.

The spatial distribution of the tapetum varies with light adaptation in *C. plumbeus*. In the dark-adapted eye, the reflective tapetum is visible across the entire fundus. Following light adaptation, the tapetum becomes partially occluded at the dorsal and ventral margins. Tapetal cells are occluded in the light-adapted state *via* the migration of melanosomes towards the retina to occlude the anterior surface of the tapetal cells (Fig. 8A–C). Spatial coverage of the tapetum over the fundus in the eye of *S. mitsukurii* is not shown to change with light adaptation and, in the light-adapted eye of *S. mitsukurii*, melanosomes only partially occlude the anterior surface of the tapetal cell (Fig. 8D).

DISCUSSION

The eyes of *S. mitsukurii* are orientated dorso-laterally within the chondrocranium (Fig. 1) and show a dorsal binocular overlap (Litherland et al., 2009), indicating that this species places particular importance on sampling the water column above. This eye orientation suggests that *S. mitsukurii* employs a visual strategy to maximise photon capture of the downwelling sunlight, possibly to detect the silhouettes of objects passing overhead. Analogous eye designs to those observed in *S. mitsukurii* are found in bony fishes inhabiting the dim light environment of the continental slopes (Locket, 1977; Lythgoe, 1979; Pankhurst, 1987). By contrast, the lateral eye position in *C. plumbeus* implies that visual sampling of the lateral and frontal water column is of particular importance for this species (Fig. 1) (Litherland et al., 2009). This eye position suggests that a visual strategy that maximises the contrast of objects (prey or predators) against the blue or blue–green backdrop of the water column is an important visual task. These visual strategies are being tested further in concurrent investigations of retinal specialisations and photon capture (Litherland et al., 2009).

The eyes of *S. mitsukurii* and *C. plumbeus* show continual growth throughout their life (Fig. 2), and the size of the eye and lens in *S. mitsukurii* is comparatively larger than in *C. plumbeus* (Fig. 2). Relative eye size has been found to vary between elasmobranch species from different habitats (Lisney and Collin, 2007). The current findings support the notion that benthic-associated sharks occupying the mesopelagic realm (i.e. *S. mitsukurii*) have relatively larger eyes than sharks occupying coastal or epipelagic realms (i.e. *C. plumbeus*) (Lisney and Collin, 2007). A large eye increases retinal illumination, an important visual strategy for species like *S. mitsukurii*, which encounter a dim light environment in mesopelagic waters.

Focal properties of the eye

Lens shape in *C. plumbeus* varies with ontogenetic growth of the eye (Fig. 2). The latero-medially flattened lens of juvenile *C. plumbeus* compares favourably with an earlier investigation of lens shape in the same species (Sivak, 1976) (15% *vs* 16% difference between lens axes). However, in adults, the lens is closer to spherical (6.5% difference between lens axes). Similarly, lens shape becomes less elliptical with ontogenetic growth in the skate, *Raja eglanteria* (Sivak and Luer, 1991), and the bamboo shark, *Chiloscyllium punctatum* (Harahush, 2009). No significant variation in lens shape occurs with ontogenetic growth of the eye in *S. mitsukurii* (Fig. 2). This implies that any variation in lens shape in elasmobranch fishes is not simply the result of pre-programmed ontogenetic growth but is species-specific and most likely reflects differing visual requirements associated with image resolution and lenticular aberrations. Elasmobranch lens shape is reported to vary between spherical, near-spherical and elliptical (Sivak, 1978a; Sivak, 1991; Sivak and Luer, 1991; Lisney, 2004). These descriptions are frequently based on an individual size class and therefore should be interpreted with some caution given the current finding that lens shape may vary as a function of growth in some species.

The lens focal length is longer than the distance measured in cryosectioned eyes between the lens centre and the retina–choroid border. We suggest the muscle responsible for lens movement in sharks (the protractor lentis muscle) may have relaxed *post-mortem* prior to our analysis of the focal distance in the cryosectioned eye and contributed to the apparent hyperopic condition of the eyes

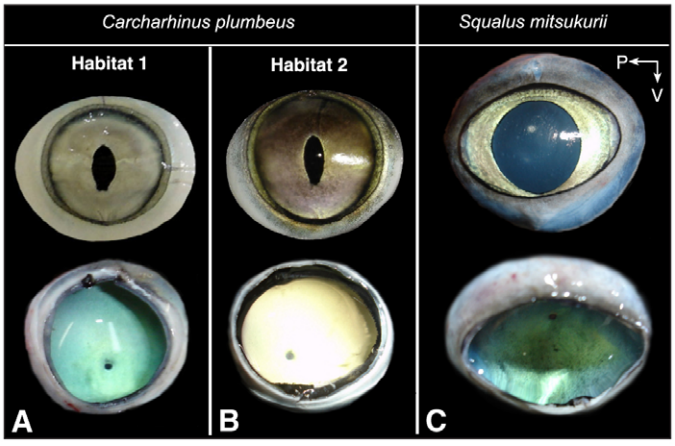

Fig. 7. Ocular pigmentation and tapetal reflectance for (A) *C. plumbeus*$_{H1}$ (an insular shelf population, depth >70 m, transparent blue water), (B) *C. plumbeus*$_{H2}$ (a coastal estuary population, depth <10 m, turbid water) and (C) *S. mitsukurii* (insular shelf population, depth >300 m, transparent blue water). P=posterior, V=ventral.

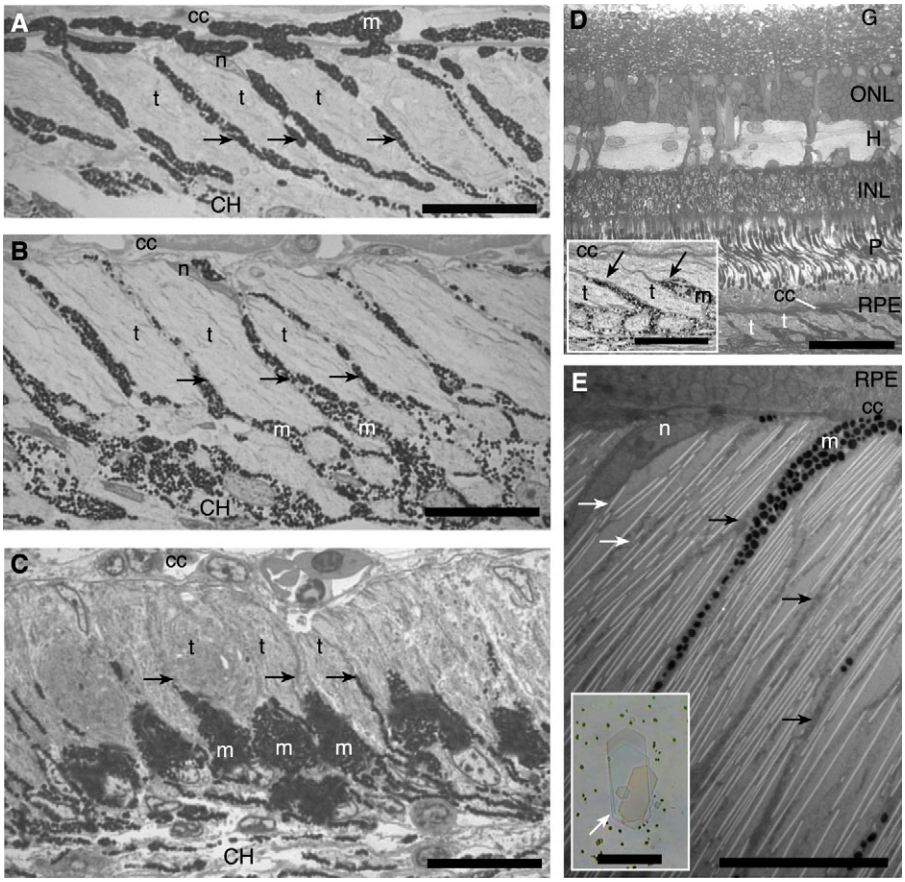

Fig. 8. Morphological variation in tapetal structure. (A–C) Light micrographs of the tapetum lucidum of *C. plumbeus* showing the occlusion of the tapetal cells by pigment migration from a light-adapted (LA) tapetum (A), a partially dark-adapted tapetum (B) and a fully dark-adapted (DA) tapetum (C). Note the dispersal of the melanosomes along the melanocyte cell processes towards the choriocapillaris in the LA state to occlude the tapetal cells and the aggregation of the melanosomes along the choroidal edge of the tapetal cells in the DA state. Scale bar, 20 μm. (D) Transverse section of the retina and tapetum in *S. mitsukurii*. Inset highlights the tapetal cells. Scale, 50 μm; inset scale, 20 μm. (E) High-power electron micrograph to illustrate the arrangement of the reflective crystals within a *C. plumbeus* tapetal cell. Inset shows a light micrograph of crystal plates. Scale bars, 10 μm. Black arrows indicate melanocyte processes, and white arrows indicate reflective crystals. Abbreviations: cc, choriocapillaris; CH, choroid; G, ganglion cell layer; H, horizontal cells; INL, inner nuclear laye; m, melanocytes containing melanosomes; n, nucleus of tapetal cell; ONL, outer nuclear layer; P, photoreceptor layer; rc, reflective crystals; RPE, retinal pigment epithelium; t, tapetal cell.

(Sivak, 1978b). Accommodative studies on a range of elasmobranchs, including *C. plumbeus*, have revealed that anaesthesia or physical restraint induces a hyperopic state of visual focus (Sivak, 1976; Sivak and Gilbert, 1976; Hueter et al., 2001). Under natural conditions, the lens should maintain a protracted (forward) position, which would allow the lens to form a focused image on the retinal plane, i.e. an emmetropic state of visual focus.

The ratio between focal length and lens size directly influences the spatial resolution and optical sensitivity of the eye, so differences in this optical parameter may reflect the visual strategies used by each species. The higher range in focal ratio in *C. plumbeus* (2.7:1 to 3.3:1) selectively enhances image magnification, and thus spatial resolution, while the lower range in focal ratio in *S. mitsukurii* (2.4:1 to 2.9:1) reflects the importance of retinal illumination and therefore light sensitivity (Fernald, 1988).

Focal ratio decreases with eye growth in both *C. plumbeus* and *S. mitsukurii* (Fig. 3), contradicting reports that focal ratio typically scales with lens growth in aquatic animals (Fernald and Wright, 1985). A decreasing focal ratio with eye growth is noted in two other elasmobranch species (Sivak and Luer, 1991; Harahush, 2009) and a few teleost fishes (Shand et al., 1999; Kröger et al., 2001; McPherson, 2004). Interestingly, the range in focal ratio observed between elasmobranch species (2.3–3.3) (Sivak, 1978a; Hueter, 1980; Hueter and Gruber, 1980; Lisney, 2004; Lisney and Collin, 2004) covers a similar range to that shown between the ontogenetic size ranges investigated in *C. plumbeus* (2.7–3.3) and *S. mitsukurii* (2.5–2.9). While species differences in focal ratio may exist, these results caution that some differences in focal ratio, as previously shown between elasmobranch species, may be an artefact of indiscriminate sampling of different sized animals.

In the absence of direct ocular measurements, Matthiessen's hypothetical focal ratio (2.55) is often used to predict values of focal length for calculations of visual acuity in elasmobranchs (Collin, 1988; Bozzano and Collin, 2000; Lisney, 2004; Litherland and Collin, 2008). Matthiessen's hypothetical focal ratio assumes a spherical lens and constant focal proportions throughout growth (Matthiessen, 1882), so this constant may not appropriately predict the focal length of elasmobranch lenses. In both *C. plumbeus* and *S. mitsukurii,* Matthiessen's hypothetical focal ratio misrepresents focal length in juvenile sharks (i.e. 60 cm TL) (Fig. 3). However, the use of Matthiessen's hypothetical ratio to predict focal length for calculations of visual acuity in larger (i.e. 186 cm TL adult) sharks appears appropriate in the absence of direct measurements of focal length.

Optical quality of the lens and its implications for vision

The lens is the only significant refractive element in most aquatic eyes and, to effectively focus light onto the retina, the lens has become almost spherical with a refractive index gradient (Sivak, 1978b; Land and Nilsson, 2002). The increased radius of curvature creates an optical problem, where light rays striking the peripheral lens will not converge with rays passing through the lens centre. In aquatic animals, variation in the refractive index gradient can control for variation in focal length between these central and peripheral light rays (longitudinal spherical aberration, LSA) (Land and Nilsson, 2002). The absence of significant amounts of LSA in any size lens of *S. mitsukurii* and *C. plumbeus* (Fig. 4) suggests that a gradient of refractive index is maintained during lens growth in elasmobranchs (Fernald and Wright, 1983; Sivak, 1991; Sivak and Luer, 1991). Lens focal properties in the eyes of other elasmobranch

species range from negative spherical aberration (central beams focus closer to the lens than the peripheral beams), as observed in *Negaprion brevirostris* (Sivak, 1991) and *Squalus acanthias* (Sivak, 1978a), to the well-corrected lenses of *Raja eglanteria* (Sivak, 1985).

The lenses of *S. mitsukurii* and *C. plumbeus* are well corrected for longitudinal chromatic aberration (LCA) between the wavelengths of 650 nm and 532 nm. LCA in other elasmobranchs is considered minimal, i.e. less than 1% of focal length for *N. brevirostris* (Hueter, 1980) and *R. eglanteria* (Sivak and Luer, 1991), although some variation in focal length between red and blue wavelengths is described for *S. acanthias* (Sivak, 1978a). LCA may be controlled for by a multifocal optical system, where subtle variations in LSA partially correct LCA (Kroger et al., 1999; Karpestam et al., 2007; Gustafsson et al., 2008), but this optical strategy has not yet been established for elasmobranchs. Multifocal optics have been described for lampreys (Gustafsson et al., 2008) and bony fish (Malkki and Kroger, 2005; Karpestam et al., 2007) and are thought to have originated early in vertebrate evolution, but further work is necessary to determine if sharks have retained a multifocal optical system. LCA is greatest for short wavelengths of light (blue–ultraviolet), so it is possible that LCA may occur at wavelengths below the spectral range investigated in this study. Short wavelength image defocus would, however, be somewhat controlled by the transmission properties of the ocular media, which are opaque to wavelengths below 400 nm (juvenile and adult *S. mitsukurii*) and below 310 nm and 382 nm for juvenile (65 cm TL) and adult (142 cm TL) *C. plumbeus*, respectively (Fig. 5).

Short wavelength-filtering ocular media, as shown in *S. mitsukurii* (Fig. 5) (Losey et al., 2003), have been found in other elasmobranch species including the wobbegong shark *Orectolobus ornatus* (T_{50}=403 nm) (Siebeck and Marshall, 2001), the grey reef shark, *C. amblyrhynchos* (T_{50}=400 nm) (Losey et al., 2003), and several batoid species (T_{50}=402–437 nm) (Siebeck and Marshall, 2001; Theiss et al., 2007). The light-filtering properties of the ocular media are attributed to a group of UV-absorbing pigments called mycosporine-like amino acids (MAAs), one of which, asterina-330, has been identified in shark lenses (Dunlap et al., 1989; Douglas and Marshall, 1999). Short-wavelength-filtering ocular media can be advantageous for species inhabiting bright light environments, as UV radiation is damaging to ocular tissue (Walls and Judd, 1933; Dunlap et al., 1989; Douglas and Marshall, 1999; Lesser et al., 2001; Zagarese and Williamson, 2001). However, unless *S. mitsukurii* undergoes vertical migrations from its deep-water habitat into shallow water, photo-protection from UV light appears an unnecessary adaptation (Frank and Widder, 1996). Apart from having a photo-protective function, short-wavelength filters may serve to enhance optical contrast for deep-water species. *S. mitsukurii* preys on mesopelagic fish, crustaceans and cephalopods (Wilson and Seki, 1994; Graham, 2005) and, in the mesopelagic zone, many of these prey species use bioluminescent light as a camouflage strategy to mimic downwelling daylight (Denton et al., 1972; Denton et al., 1985). Short-wavelength opaque lenses can enhance the contrast difference between downwelling daylight and the broader blue–green spectrum of the bioluminescent light and so facilitate the visual detection of prey silhouettes (Muntz, 1976a; Somiya, 1976; Denton et al., 1985; Warrant and Locket, 2004). A similar function has been attributed to the short-wavelength opaque lenses found in several species of mesopelagic fish (Muntz, 1976a; Somiya, 1976; Somiya, 1982; Douglas and Thorpe, 1992; Warrant and Locket, 2004).

Ocular spectral transmission can vary with the extent of exposure to UV light in elasmobranchs (Nelson et al., 2003). However, this study did not detect any difference in lenticular filtering between juveniles sampled from populations inhabiting a shallow estuary (*C. plumbeus*$_{H2}$) and the deeper waters of an oceanic insular shelf (*C. plumbeus*$_{H1}$) (Fig. 5). Turbid water, such as that inhabited by *C. plumbeus*$_{H2}$, could reduce exposure to high levels of short-wavelength light, resulting in a similar level of UV exposure for these separate populations of juveniles.

The transmission properties of the ocular media of *C. plumbeus*$_{H1}$ did vary as a function of lens size, which may explain the contradictory reports from earlier investigations that have described the lenses of *C. plumbeus* to be both unpigmented (Losey et al., 2003) and pigmented (Zigman, 1991). Ontogenetic change in ocular spectral transmissions may occur in response to an increased exposure to UV light between juveniles and adults or, alternatively, may occur because larger lenses absorb a greater proportion of short-wavelength radiation than smaller lenses (Thorpe and Douglas, 1993). Although, intra-specific variation in UV-absorbing pigment concentration is thought to be minimal in other carcharhinid sharks (Dunlap et al., 1989), another elasmobranch species, the giant shovelnose ray, *Rhinobatos batillum* (=*Glaucostegus typus*), similarly shows ontogenetic variation in ocular media spectral transmission (Siebeck and Marshall, 2001), as do some coral reef fish (Nelson et al., 2003). Lens spectral transmission properties of adult (142 cm TL) *C. plumbeus* are, however, comparable with the closely related dusky shark, *Carcharhinus obscurus* (absorption max=360 nm) (Zigman, 1991), and the scalloped hammerhead, *Sphyrna lewini* (T_{50}=385 nm) (Losey et al., 2003), where both species occupy similar depth ranges to adult *C. plumbeus* (Compagno et al., 2005).

C. plumbeus places particular importance on sampling the horizontal visual field (Litherland et al., 2009). The more UV-transparent ocular media of *C. plumbeus* (juveniles and adults), compared with *S. mitsukurii*, may therefore enhance the visual sensitivity of the eye in the restricted spectral range of the horizontal visual field in the marine light environment (Muntz, 1976b; McFarland, 1990; Douglas and Thorpe, 1992; Losey et al., 1999). A negative trade-off is an increased susceptibility to UV damage of ocular tissues; so, smaller sharks (which have more transparent lenses) may favour habitats with diminished levels of short-wavelength light such as deep or turbid water.

Characteristics of the tapetum lucidum

The design of the choroidal tapetum of *S. mitsukurii* and *C. plumbeus* is similar to that of other elasmobranchs, where overlapping tapetal cells are interdigitated by melanocytes containing melanosomes that migrate in response to light (Fig. 8). In *C. plumbeus*, the size of the tapetal cell varies across the eyecup (5–30 μm), with those cells occurring in the central retina being much broader compared with the tapetal cells of other elasmobranchs (3–6 μm) (Bernstein, 1961; Denton and Nicol, 1964; Nicol, 1964; Denton and Nicol, 1965a; Best and Nicol, 1967; Kuchnow, 1969; Heath, 1991; Braekevelt, 1994a) (L.L., unpublished). The tapetal cells of both species contain layers of reflective crystals and, based on previous studies of the elasmobranch tapetum, these are assumed to be comprised of guanine (Denton and Nicol, 1964). The size and structure of the reflective crystals are comparable with those of other elasmobranchs (0.1 μm thick, 5–8 μm long) (Braekevelt, 1991; Braekevelt, 1994a; Braekevelt, 1994b) (L.L., unpublished). In addition, the number of reflective layers contained within each tapetal cell (8–25) lies approximately within the range reported for other elasmobranch species (9–20) (Bernstein, 1961; Denton and Nicol, 1964; Nicol, 1964; Denton and Nicol, 1965a; Best and Nicol,

1967; Kuchnow, 1969; Heath, 1991; Braekevelt, 1994a) (L.L., unpublished). The lowest number of crystal layers per tapetal cell is observed where multiple tapetal cells overlap, such that, at any location, the tapetal layer consists of more than 20 layers of reflective material, producing a reflectance that would theoretically approach 100% (Land, 1972).

Eyeshine, or the coloured reflection elicited by the fundus, may be tuned to match the predominant spectrum of light available in an animal's habitat (Douglas et al., 1998). The blue coloured tapeta of *S. mitsukurii* would principally reflect the shorter wavelength light (blue–green) that penetrates the mesopelagic zone, including that emitted as bioluminescence (Tyler and Smith, 1970; Warrant and Locket, 2004). Intra-specific differences in the eyeshine of *C. plumbeus* suggest that the light reflected by the tapetum is tuned according to the ambient light environment. The blue tapetal reflectance of *C. plumbeus*$_{H1}$ closely matches the predominant blue background light of an oceanic insular shelf and fringing reef (Marshall et al., 2003), and the orange–green reflectance of *C. plumbeus*$_{H2}$ is consistent with the predominant spectrum of light in a turbid estuary and shallow coastal waters (Lythgoe, 1979; Schubert et al., 2001). The ability to vary tapetal spectral reflectance in *C. plumbeus* may be an adaptation to match ambient illumination (with respect to both intensity and spectral composition) in a variety of light environments for the purposes of camouflage in addition to increasing retinal illumination. Evidence that tapetal reflectance may be tuned to match the predominant wavelength spectrum of a species' habitat in elasmobranchs and teleosts has been suggested previously (Best and Nicol, 1967). Tapetal reflectance is produced by constructive interference (Denton and Nicol, 1964; Denton and Nicol, 1965b) such that differences in the crystal width and inter-crystal spacing within the tapetal cells provide a mechanism to vary the spectral composition of the reflected light (Braekevelt, 1994a). The current study did reveal variations in inter-crystal spacing (0.2–0.7 μm) but these were not significant between the different populations of *C. plumbeus*, presumably due to the resolution afforded by the sectioning procedure in conjunction with minor variations in the sectioning angle.

Visual ecology

S. mitsukurii shows ocular adaptations specialised for vision in the dim light environment of its deep-water mesopelagic habitat. Ocular characteristics such as its relatively large eye size (Fig. 2), non-occlusible tapetum (Fig. 7), large, immobile pupillary aperture (Fig. 4) and low focal ratio translate into an eye capable of high light-gathering power (*f*-number=1.2–1.5). This visual strategy would enhance the detection and amplification of low light levels in a uniformly scattered light environment, such as encountered in the mesopelagic zone. Lenticular filters, which enhance optical contrast, are a further visual adaptation to this species' light environment since bioluminescent light becomes increasingly visible in the mesopelagic zone (Warrant and Locket, 2004). Similar optical features are documented for other deep-water sharks (Denton and Nicol, 1964), i.e. *Galeus melastomus* (Bozzano et al., 2001), *Etmopterus virens* (Gilbert, 1963), *Oxynotus centrina* and *Apristurus brunneus* (Kuchnow, 1971). Optical parameters of *S. mitsukurii* show minimal variation with growth, which intuitively suggests that visual requirements of juvenile and adult *S. mitsukurii* are quite similar. Information on diet and spatial distribution for this species is limited, although juveniles and adults can be caught in the same location (L.L., personal observation). Given that the optical features of *S. mitsukurii* are designed for low light levels, unnatural exposure to bright light, such as that resulting from fishing activities (i.e. daylight or deck-lights), may impair visual function (Wu et al., 2006; Brill et al., 2008) and hence impact on this species' post-release survival if caught as by-catch, for example, in trawl fisheries (Graham et al., 2001) by impeding its ability to avoid predation and/or capture prey for some period after its release.

C. plumbeus shows an ability to adapt its ocular components to optimise vision in diverse light environments. Eye structure in *C. plumbeus* changes with eye growth, implying that visual performance changes between life-history stages. This may reflect the dietary shift from benthic-associated, less-mobile prey (i.e. crustaceans) as juveniles to larger more-mobile prey items (i.e. large schooling pelagic fish) as adults (Medved et al., 1985; Ellis, 2003; McElroy et al., 2006). Furthermore, an iris capable of rapid changes in pupil size (Fig. 6) (Gilbert et al., 1981), an occlusible tapetum and a variable *f*-number (2.0–6.0) provide a dynamic mechanism to regulate retinal illumination (Kuchnow and Martin, 1970; Kuchnow, 1971; Gilbert et al., 1981; Sivak and Luer, 1991). These visual characteristics would help maintain optimal visual performance in fluctuating lighting conditions, such as are encountered in a shallow estuary (Schubert et al., 2001) or during vertical movements through the upper water column. Importantly, these characteristics may afford *C. plumbeus* with some ability to adapt to anthropogenic environmental modifications of their coastal habitat, such as light pollution or increased water turbidity.

In summary, the light environment appears to strongly influence optical design in this class of vertebrates. Throughout a shark's life, the nature of visual scenes may change and, with it, the optical adaptations of the visual sense. It is pertinent then that future investigations of visual function in elasmobranchs account for ontogenetic variability in ocular parameters. *C. plumbeus* and *S. mitsukurii* are well equipped to perform visual tasks in the specific light environment of their respective microhabitats. These findings highlight the importance of visual information to the sensory world of sharks.

LIST OF ABBREVIATIONS

A	anterior
A_{max}	maximum pupillary aperture
D	dorsal
DA	dark adapted
fr	focal ratio
LA	light adapted
LCA	longitudinal chromatic aberration
LSA	longitudinal spherical aberration
P	posterior
T_{50}	wavelength at which 50% of incident light is transmitted
TL	total length
V	ventral

R. Brill and K. Holland provided generous logistical support and assistance with field operations. T. S. Daly-Engel, A. Horodysky, D. Grubbs, C. Magel, P. Kingsley-Smith, L. Pace, P. Bushnell, staff of the VIMS Eastern Shore Laboratory, captains and crews of Silversea, PameLa J and CJDJ provided resourceful assistance with field operations, specimen collection and elasmobranch husbandry. F. Kandel and U. Siebeck generously assisted with ocular media measurements. L. Tolley provided histological expertise. L. Litherland is an Australian Postgraduate Awardee and a CSIRO Postgraduate Scholarship Awardee 2005–2008, with further project funding supplied by Project AWARE.

REFERENCES

Bernstein, M. H. (1961). The tapetum of the dogfish eye and the mechanism of dark adaptation. *Anat. Rec.* **139**, 208.

Best, A. C. G. and Nicol, J. A. C. (1967). Reflecting cells of the elasmobranch tapetum lucidum. *Contrib. Mar. Sci.* **12**, 172-201.

Bozzano, A. and Collin, S. P. (2000). Retinal ganglion cell topography in elasmobranchs. *Brain. Behav. Evol.* **55**, 191-208.

Bozzano, A., Murgia, R., Vallerga, S., Hirano, J. and Archer, S. (2001). The photoreceptor system in the retinae of two dogfishes, *Scyliorhinus canicula* and

Galeus malastomus: possible relationship with the depth distribution and predatory lifestyle. *J. Fish. Biol.* **59**, 1258-1278.
Braekevelt, C. R. (1991). Electron microscopic study of the occlusible tapetum lucidum of the southern fiddler ray (*Trygonorhina fasciata*). *Histol. Histopathol.* **6**, 509-514.
Braekevelt, C. R. (1994a). Fine structure of the choroidal tapetum lucidum in the Port Jackson shark (*Heterodontus phillipi*). *Anat. Embryol.* **190**, 591-596.
Braekevelt, C. R. (1994b). Fine structure of the tapetum lucidum in the short-tailed stingray (*Dasyatis brevicaudata*). *Histol. Histopathol.* **9**, 495-500.
Brill, R., Magel, C., Davis, M., Hannah, R. and Rankin, P. (2008). Effects of rapid decompression and exposure to bright light on visual function in black rockfish (*Sebastes melanops*) and Pacific halibut (*Hippoglossus stenolepis*). *Fish. Bull.* **106**, 427-437.
Cliff, G., Dudley, S. F. J. and Davis, B. (1988). Sharks caught in the protective gill nets off Natal, South Africa.1. The Sandbar Shark *Carcharhinus plumbeus* (Nardo). *S. Afr. J. Mar. Sci.* **7**, 255-265.
Cohen, J. L. (1982). Vision in sharks. *Oceanus* **24**, 17-22.
Collin, S. P. (1988). The retina of the shovel-nosed ray, *Rhinobatos batillum* (Rhinobatidae): morphology and quantitative analysis of the ganglion, amacrine and bipolar cell populations. *J. Exp. Biol.* **47**, 195-207.
Compagno, L. J. V., Dando, M. and Fowler, S. (2005). *A Field Guide to the Sharks of the World.* London: Collins.
Costantini, M. and Affronte, M. (2003). Neonatal and juvenile sandbar sharks in the northern Adriatic Sea. *J. Fish. Biol.* **62**, 740-743.
Daly-Engel, T. S., Grubbs, R. D., Bowen, B. W. and Toonen, R. J. (2007). Frequency of multiple paternity in an unexploited tropical population of sandbar sharks (*Carcharhinus plumbeus*). *Can. J. Fish. Aquat. Sci.* **64**, 198-204.
Denton, E. J. and Nicol, J. A. C. (1964). The choroidal tapeta of some cartilaginous fishes (chondrichthyes). *J. Mar. Biol. Assoc. U.K.* **44**, 219-258.
Denton, E. J. and Nicol, J. A. C. (1965a). Direct measurements of the orientation of the reflecting surfaces in the tapetum of *Squalus acanthias* and some observations on the tapetum of *Acipenser sturio*. *J. Mar. Biol. Assoc. U.K.* **45**, 739-742.
Denton, E. J. and Nicol, J. A. C. (1965b). Studies on reflexion of light from silvery surfaces of fishes, with special reference to the bleak, *Alburnus alburnus*. *J. Mar. Biol. Assoc. U.K.* **45**, 683-703.
Denton, E. J., Gilpin-Brown, J. B. and Wright, P. G. (1972). The angular distribution of the light produced by some mesopelagic fish in relation to their camouflage. *Proc. R. Soc. Lond. B.* **182**, 145-158.
Denton, E. J., Herring, P. J., Widder, E. A., Latz, M. F. and Case, J. F. (1985). The roles of filters in the photophores of oceanic animals and their relation to vision in the oceanic environment. *Proc. R. Soc. Lond. B.* **225**, 63-97.
Douglas, R. H. and Marshall, N. J. (1999). A review of vertebrate and invertebrate ocular filters. In *Adaptive Mechanisms in the Ecology of Vision* (ed. S. N. Archer, B. A. Djamgoz, E. R. Loew, J. C. Partridge and S. Vallerga), pp. 95-162. Dordrecht: Kluwer.
Douglas, R. H. and McGuigan, C. M. (1989). The spectral transmission of freshwater teleost ocular media-an interspecific comparison and a guide to potential ultraviolet sensitivity. *Vision Res.* **29**, 871-879.
Douglas, R. H. and Thorpe, A. (1992). Short-wave absorbing pigments in the ocular lenses of deep-sea teleosts. *J. Mar. Biol. Assoc. U.K.* **72**, 93-112.
Douglas, R. H., Partridge, J. C. and Marshall, N. J. (1998). The eyes of deep-sea fish. I. Lens pigmentation, tapeta and visual pigments. *Prog. Retin. Eye Res.* **17**, 587-636.
Dunlap, W. C., Williams, D. M., Chalker, B. and Banaszak, A. T. (1989). Biochemical photoadaptation in vision: UV absorbing pigments in fish eye tissues. *Comp. Biochem. Physiol.* **93B**, 601-607.
Ellis, J. K. (2003). Diet of the sandbar shark, *Carcharhinus plumbeus*, in the Chesapeake Bay and adjacent waters. MSc. Thesis. The College of William and Mary in Virginia, Gloucester, USA.
Fern, D. (2004). Optics and retinal anatomy of the brown banded bamboo shark, *Chiloscyllium punctatum.* Bsc. Thesis. The University of Queensland, Brisbane, Australia.
Fernald, R. D. (1988). Aquatic adaptations of fish eyes. In *Sensory Biology of Aquatic Animals* (ed. J. Atema, R. R. Fay, A. N. Popper and W. N. Tavolga), pp. 435-466. New York: Springer-Verlag.
Fernald, R. D. (1991). Teleost vision: seeing while growing. *J. Exp. Zool.* **Suppl. 6**, 167-180.
Fernald, R. D. and Wright, S. E. (1983). Maintenance of optical quality during crystalline lens growth. *Nature* **301**, 618-620.
Fernald, R. D. and Wright, S. E. (1985). Growth of the visual system in the African cichlid fish *Haplochromis burtoni*: optics. *Vision Res.* **25**, 155-161.
Frank, T. M. and Widder, E. A. (1996). UV light in the deep-sea: in situ measurements of downwelling irradiance in relation to the visual threshold sensitivity of UV-sensitive crustaceans. *Mar. Freshw. Behav. Physiol.* **27**, 189-197.
Gilbert, P. W. (1963). The visual apparatus of sharks. In *Sharks and Survival* (ed. P. W. Gilbert), pp. 283-326. Boston: D. C. Health and Co.
Gilbert, P. W., Sivak, J. G. and Pelham, R. E. (1981). Rapid pupil change in selachians. *Can. J. Zool.* **59**, 560-564.
Graham, K. G. (2005). Distribution, population structure and biological aspects of *Squalus* spp. (Chondrichthyes: Squaliformes) from New South Wales and adjacent Australian waters. *Mar. Freshwater. Res.* **56**, 405-416.
Graham, K. J., Andrew, N. L. and Hodgson, K. E. (2001). Changes in relative abundance of sharks and rays on Australian South East Fishery trawl grounds after twenty years of fishing. *Mar. Freshw. Res.* **52**, 549-561.
Grubbs, R. D., Musick, J. A., Conrath, C. and Romine, J. G. (2007). Long-term movements, migrations, and temporal delineation of a summer nursery for juvenile sandbar sharks in the Chesapeake Bay region. *Am. Fish. Soc. Symp.* **50**, 63-86.
Gustafsson, O. S. E., Collin, S. P. and Kroger, R. H. H. (2008). Early evolution of multifocal optics for well-focused colour vision in vertebrates. *J. Exp. Biol.* **211**, 1559-1564.
Harahush, B. K. (2009). Ontogenetic changes in the visual system of the brown banded bamboo shark, *Chiloscyllium punctatum* (Elasmobranchii), with special reference to husbandry and breeding. PhD Thesis. The University of Queensland, Brisbane, Australia.
Hart, S. N., Lisney, T. J. and Collin, S. P. (2006). Visual communication in elasmobranchs. In *Communication in Fishes* (ed. F. Ladich, S. P. Collin, P. Moller and B. G. Kapoor), pp. 337-372. Plymouth: Science Publishers.
Heath, A. R. (1991). The ocular tapetum lucidum: a model system for interdisciplinary studies in elasmobranch biology. *J. Exp. Zool.* **Suppl. 5**, 41-45.
Herring, P. J. (1996). Light, colour and vision in the ocean. In *Oceanography: An Illustrated Guide* (ed. C. P. Summerhayes and S. A. Thorpe), pp. 212-227. London: Mason Publishing.
Hueter, R. E. (1980). Physiological optics of the eye of the juvenile lemon shark (*Negaprion brevirostris*). MSc. Thesis. University of Miami, FL, USA.
Hueter, R. E. (1991). Adaptations for spatial vision in sharks. *J. Exp. Zool.* **Suppl. 5**, 130-141.
Hueter, R. E. and Gruber, S. H. (1980). Retinoscopy of aquatic eyes. *Vision Res.* **20**, 197-200.
Hueter, R. E., Murphy, C. J., Howland, M., Sivak, J. G., Paul-Murphy, J. R. and Howland, H. C. (2001). Refractive state and accommodation in the eyes of free-swimming versus restrained juvenile lemon sharks (*Negaprion brevirostris*). *Vision Res.* **41**, 1885-1889.
Joung, S. J. and Chen, C. T. (1995). Reproduction in the sandbar shark, *Carcharhinus plumbeus*, in the waters off northeastern Taiwan. *Copeia* **1995**, 659-665.
Joung, S. J., Liao, Y. Y. and Chen, C. T. (2004). Age and growth of sandbar shark, *Carcharhinus plumbeus*, in northeastern Taiwan waters. *Fish. Res.* **70**, 83-96.
Karpestam, B., Gustafsson, J., Shashar, N., Katzir, G. and Kroger, R. H. H. (2007). Multifocal lenses in coral reef fishes. *J. Exp. Biol.* **210**, 2923-2931.
Kroger, R. H. H., Cambell, M. C. W., Munger, R. and Fernald, R. D. (1994). Refractive index distribution and spherical aberration in the crystalline lens of the African cichlid fish *Haplochromis burtoni*. *Vision Res.* **34**, 1815-1822.
Kroger, R. H. H., Cambell, M. C. W., Fernald, R. D. and Wagner, H. J. (1999). Multifocal lenses compensate for chromatic defocus in vertebrate eyes. *J. Comp. Physiol. A* **184**, 361-369.
Kröger, R. H., Campbell, M. C. and Fernald, R. D. (2001). The development of the crystalline lens is sensitive to visual input in the African cichlid fish, *Haplochromis burtoni*. *Vision Res.* **41**, 549-559.
Kuchnow, K. P. (1969). Tapetal pigment response of elasmobranchs. *Vision Res.* **9**, 849-854.
Kuchnow, K. P. (1971). Elasmobranch pupillary response. *Vision Res.* **11**, 1395-1397.
Kuchnow, K. P. and Martin, R. (1970). Pigment migration in tapetum lucidum of elasmobranch eye: evidence for a nervous mechanism. *Vision Res.* **10**, 825-827.
Land, M. F. (1972). The physics and biology of animal reflectors. *Prog. Biophys. Mol. Biol.* **24**, 75-106.
Land, M. F. and Nilsson, D. E. (2002). *Animal Eyes.* Oxford: Oxford University Press.
Lesser, M. P., Turtle, S. L., Farrell, J. H. and Walker, C. W. (2001). Exposure to ultraviolet radiation (290-400 nm) causes oxidative stress, DNA damage, and expression of p53/p73 in laboratory experiments on embryos of the spotted salamander, *Ambystoma maculatum*. *Physiol. Biochem. Zool.* **74**, 733-741.
Lisney, T. J. (2004). Neuroethology and vision in elasmobranchs. PhD. Thesis. The University of Queensland, Brisbane, Australia.
Lisney, T. J. and Collin, S. P. (2004). Matthiessen's ratio and lens shape in elasmobranches. In *Proceedings of the Australian Neuroscience Society Annual Conference 27–30 January 2004 (84-84).* Australian Neuroscience Society Inc., Melbourne, Australia.
Lisney, T. J. and Collin, S. P. (2007). Relative eye size in elasmobranchs. *Brain. Behav. Evol.* **69**, 266-279.
Litherland, L. and Collin, S. P. (2008). Comparative visual function in elasmobranchs: spatial arrangement and ecological correlates of photoreceptor and ganglion cell distributions. *Vis. Neurosci.* **25**, 549-561.
Litherland, L., Collin, S. P. and Fritsches, K. A. (2009). Eye growth in sharks: Ecological implications for changes in retinal topography and visual resolution. *Vis. Neurosci.,* doi:10.1017/S0952523809990174. Published online by Cambridge University Press, 26 August 2009.
Locket, N. A. (1977). Adaptations to the deep sea environment. In *Handbook of Sensory Physiology*, vol. VII/5 (ed. F. Crescitelli), pp. 68-192. Berlin: Springer Verlag.
Losey, G. S., Cronin, T. W., Goldsmith, T. H., Hyde, D., Marshall, N. J. and McFarland, W. N. (1999). The UV visual world of fishes: a review. *J. Fish. Biol.* **54**, 921-943.
Losey, G. S., McFarland, W. N., Loew, E. R., Zamzow, J. P., Nelson, P. A. and Marshall, N. J. (2003). Visual biology of Hawaiian coral reef fishes. I. Ocular transmission and visual pigments. *Copeia* **2003**, 433-454.
Lythgoe, J. N. (1979). *The Ecology of Vision.* Oxford: Oxford University Press.
Malkki, P. E. and Kroger, R. H. H. (2005). Visualisation of chromatic correction of fish lenses by multiple focal lengths. *J. Opt. A* **7**, 691-700.
Marshall, N. J., Jennings, K., McFarland, W. N., Loew, E. R. and Losey, G. S. (2003). Visual biology of Hawaiian coral reef fishes. III. Environmental light and an integrated approach to the ecology of reef fish vision. *Copeia* **2003**, 467-480.
Matthiessen, L. (1882). Über die Beziehung, welche zwischen dem Brechungsindex des Kernzentrums der Kristallinse und den Dimensionen des Auges bestehen. *Pflügers Arch.* **27**, 510-523.
McAuley, R., Lenanton, R., Chidlow, J., Allison, R. and Heist, E. (2005). Biology and stock assessment of the thickskin (sandbar) shark, *Carcharhinus plumbeus*, in Western Australia and further refinement of the dusky shark, *Carcharhinus obscurus*, stock assessment. Final Fisheries Research and Development Corporation Report - Project 2000/134, Fisheries Research Report No. 151, Department of Fisheries, Western Australia, 132pp.

McAuley, R. B., Simpfendorfer, C. A., Hyndes, G. A. and Lenanton, R. C. J. (2007). Distribution and reproductive biology of the sandbar shark, *Carcharhinus plumbeus* (Nardo), in Western Australia waters. *Mar. Freshw. Res.* **58**, 116-126.
McElroy, W. D., Wetherbee, B. M., Mostello, C. S., Lowe, C. G., Crow, G. L. and Wass, R. C. (2006). Food habits and ontogenetic changes in the diet of the sandbar shark, *Carcharhinus plumbeus*, in Hawaii. *Envir. Biol. Fish.* **76**, 81-92.
McFarland, W. (1990). Light in the sea-the optical world of elasmobranchs. *J. Exp. Zool.* **Suppl. 5**, 3-12.
McPherson, K. (2004). Retinal anatomy and optics in the mackeral tuna *Euthynnus affinis*. Bsc. Thesis. University of Queensland, Brisbane, USA.
Medved, R. J., Stillwell, C. E. and Casey, J. J. (1985). Stomach contents of young sandbar sharks, *Carcharhinus plumbeus*, in Chincoteague Bay, Virginia. *Fish. Bull.* **83**, 395-402.
Muntz, W. R. A. (1976a). On yellow lenses in mesopelagic animals. *J. Mar. Biol. Assoc. U. K.* **56**, 963-976.
Muntz, W. R. A. (1976b). The visual consequences of yellow filtering pigments in the eyes of fishes occupying different habitats. In *Light as an Ecological Factor II* (ed. S. C. Evans, R. Bainbridge and O. Packham), pp. 271-287. Oxford: Blackwell Scientific.
Murphy, C. J. and Howland, H. C. (1990). The functional significance of crescent-shaped pupils and multiple pupillary apertures. *J. Exp. Zool.* **Suppl. 5**, 22-28.
Nelson, P. A., Zamzow, J. P., Erdmann, S. W. and Losey, G. S. (2003). Ontogenetic changes and environmental effects on ocular transmission in four species of coral reef fishes. *J. Comp. Physiol. A* **189**, 391-399.
Nicol, J. A. C. (1964). Reflectivity of the chorioidal tapeta of selachians. *J. Fish. Res. Board Can.* **21**, 1089-1100.
Pankhurst, N. W. (1987). Intra- and interspecific changes in retinal morphology among mesopelagic and demersal teleosts from the slope waters of New Zealand. *Envir. Biol. Fish.* **19**, 269-280.
Romine, J. G., Grubbs, R. D. and Musick, J. A. (2006). Age and growth of the sandbar shark, *Carcharhinus plumbeus*, in Hawaiian waters through vertebral analysis. *Envir. Biol. Fish.* **77**, 229-239.
Sadler, J. D. (1973). The focal length of the fish eye lens and visual acuity. *Vision Res.* **13**, 417-423.
Schubert, H., Sagert, S. and Forster, R. M. (2001). Evaluation of the different levels of variability in the underwater light field of a shallow estuary. *Helgol. Mar. Res.* **55**, 12-22.
Shand, J., Doving, K. B. and Collin, S. P. (1999). Optics of the developing fish eye: comparisons of Matthiessen's ratio and focal length of the lens in the black bream *Acanthopagrus butcheri* (Sparidae, Teleostei). *Vision Res.* **39**, 1071-1078.
Siebeck, U. E. and Marshall, N. J. (2001). Ocular media transmission of coral reef fish-can coral reef fish see ultraviolet light? *Vision Res.* **41**, 133-149.
Sivak, J. G. (1974). Accommodation of the lemon shark eye (*Negaprion brevirostris*). *Vision Res.* **14**, 215-216.
Sivak, J. G. (1976). The accommodative significance of the "ramp" retina of the eye of the stingray. *Vision Res.* **16**, 945-950.
Sivak, J. G. (1978a). Optical characteristics of the eye of the spiny dogfish (*Squalus acanthias*). *Rev. Can. Biol.* **37**, 209-217.
Sivak, J. G. (1978b). Refraction and accommodation of the elasmobranch eye. In *Sensory Biology of Sharks, Skates and Rays* (ed. E. S. Hodgson and R. F. Mathewson), pp. 107-116. Virginia, USA: Office of Naval Research Department of the Navy.
Sivak, J. G. (1985). Optics of the crystalline lens. *Am. J. Optomol. Physiol. Opt.* **62**, 299-308.
Sivak, J. G. (1991). Elasmobranch visual optics. *J. Exp. Zool.* **Suppl. 5**, 13-21.
Sivak, J. G. and Gilbert, P. W. (1976). Refractive and histological study of accommodation in 2 species of sharks *Ginglymostoma cirratum* and *Carcharhinus milberti*. *Can. J. Zool.* **54**, 1811-1817.
Sivak, J. G. and Luer, C. A. (1991). Optical development of the ocular lens of an elasmobranch, *Raja elanteria*. *Vision Res.* **31**, 373-382.
Somiya, H. (1976). Functional significance of the yellow lens in the eyes of *Argyropelecus affinis*. *Mar. Biol.* **34**, 93-99.
Somiya, H. (1982). "Yellow lens" eyes of a stomiatoid deep-sea fish, *Malcosteus niger*. *Proc. R. Soc. Lond. B* **215**, 481-489.
Springer, S. (1960). Natural history of the sandbar shark *Eulamia milberti*. *U. S. Fish. Wildl. Serv. Fish. Bull.* **61**, 1-38.
Theiss, S. M., Lisney, T. J., Collin, S. P. and Hart, N. S. (2007). Colour vision and visual ecology of the blue-spotted maskray, *Dasyatis kuhlii* Muller & Henle, 1814. *J. Comp. Physiol. A* **193**, 67-79.
Thorpe, A. and Douglas, R. H. (1993). Spectral transmission and short-wave absorbing pigments in the fish lens II. Effects of age. *Vision Res.* **33**, 301-307.
Tyler, J. E. and Smith, R. C. (1970). *Measurements of Spectral Irradiance Underwater*. New York: Gordon and Breach Science Publishers.
Walls, G. L. and Judd, H. D. (1933). The intra-ocular colour-filters of vertebrates. *Br. J. Ophthalmol.* **17**, 641-675.
Warrant, E. J. (2000). The eyes of seep-sea fishes and the changing nature of visual scenes with depth. *Philos. Trans. R. Soc. Lond. B* **355**, 1155-1159.
Warrant, E. J. and Locket, N. A. (2004). Vision in the deep sea. *Biol. Rev.* **79**, 671-712.
Wilson, C. D. and Seki, M. P. (1994). Biology and population characteristics of *Squalus mitsukurii* from a seamount in the Central North Pacific Ocean. *Fish. Bull.* **92**, 851-864.
Wu, J. Y., Seregard, S. and Algvere, P. V. (2006). Photochemical damage of the retina. *Surv. Ophthalmol.* **51**, 461-481.
Zagarese, H. E. and Williamson, C. E. (2001). The implications of solar UV radiation exposure for fish and fisheries. *Fish Fish. Ser.* **2**, 250-260.
Zigman, S. (1991). Comparative biochemistry and biophysics of elasmobranch lenses. *J. Exp. Zool.* **Suppl. 5**, 29-40.